

## MIT Open Access Articles

*Reynolds Number Effects on the Vortex-Induced Vibration of Flexible Marine Risers*

The MIT Faculty has made this article openly available. **Please share** how this access benefits you. Your story matters.

**Citation:** Resvanis, Themistocles L., Vikas Jhingran, J. Kim Vandiver, and Stergios Liapis. "Reynolds Number Effects on the Vortex-Induced Vibration of Flexible Marine Risers." Volume 5: Ocean Engineering; CFD and VIV (July 1, 2012).

**As Published:** <http://dx.doi.org/10.1115/OMAE2012-83565>

**Publisher:** American Society of Mechanical Engineers

**Persistent URL:** <http://hdl.handle.net/1721.1/109466>

**Version:** Final published version: final published article, as it appeared in a journal, conference proceedings, or other formally published context

**Terms of Use:** Article is made available in accordance with the publisher's policy and may be subject to US copyright law. Please refer to the publisher's site for terms of use.



OMAE2012-83565

## REYNOLDS NUMBER EFFECTS ON THE VORTEX-INDUCED VIBRATION OF FLEXIBLE MARINE RISERS

**Themistocles L. Resvanis**  
Massachusetts Institute of Technology  
Cambridge, Massachusetts, USA

**J. Kim Vandiver**  
Massachusetts Institute of Technology  
Cambridge, Massachusetts, USA

**Vikas Jhingran**  
Shell International Exploration & Prod. Inc  
Houston, Texas, USA

**Stergios Liapis**  
Shell International Exploration & Prod. Inc  
Houston, Texas, USA

### ABSTRACT

This paper explores the Reynolds number dependence of the Vortex-Induced Vibration (VIV) of flexible marine risers. Emphasis is placed on revealing the trends that exist between the Strouhal number and the Reynolds number and between the dimensionless amplitude ( $A/D$ ) and Reynolds number. Data is drawn from recent towing tank experiments which used flexible cylinders of three different diameters. The 38m long pipes were exposed to uniform and sheared currents. The Reynolds number range extended from approximately 5,000 to 220,000 -well into the critical regime- with the larger diameter pipes responding in up to the 13<sup>th</sup> mode and the smaller diameter pipe responding well above the 20<sup>th</sup> mode. The results and trends from this set of experiments are compared to previous results from laboratory and field experiments.

### INTRODUCTION

The Reynolds number,  $Re$ , is a very important dimensionless parameter in most fluid dynamics problems including VIV.

$$Re = \frac{U D}{\nu}$$

Recently, independent studies by Govardhan and Williamson (2006) and Klammo et al. (2005) have shown that the Reynolds number is extremely important when analyzing the response amplitude of rigid cylinders undergoing VIV in laboratory experiments. Both studies demonstrate that the mass ratio does not influence the peak response amplitude whereas there is a strong dependence on the Reynolds number - with the peak response amplitude increasing as the Reynolds number is increased.

Despite being an important factor that governs the behavior of VIV, it has been very hard to study the effect of Reynolds number on the VIV response of flexible risers. A lot of the

high Reynolds number data remains the proprietary information of the oil and gas companies that funded the experiments, and only a few published datasets are available to researchers. Furthermore, when attempting to compile enough data so as to span a reasonable Reynolds number range, one inevitably runs into the problem of comparing data from many different systems with different dynamic properties, instrumentation procedures, etc...

To date, the most comprehensive study of the Reynolds number effects on flexible cylinders is the work of Swithenbank et al (2008) who compile and organize the  $A/D$  vs.  $Re$  number data from ten different datasets including laboratory and field experiments.

This paper attempts to build on the past work by using data from recent experiments on flexible pipes where the Reynolds number range spans three orders of magnitude. The aim of this paper is to reveal the trends that exist between the Reynolds number and some of the most important VIV response parameters (Strouhal number, cross-flow ( $CF$ ) & in-line ( $IL$ ) amplitudes and drag coefficient ( $C_d$ )).

### Effect of Reynolds number on the response of rigid cylinders

Govardhan & Williamson (2006) and Klammo et al (2005) independently showed that the Reynolds number influences the peak response of a rigid cylinder free to vibrate in a cross-flow. After accounting for the Reynolds number dependence both Williamson and Klammo were able to show excellent correlation between peak response amplitudes with their respective damping parameters. The authors clearly demonstrate that the response amplitude depends on the Reynolds number and some form of damping parameter.

Vandiver (2012) reviews the history of damping parameters, including the two used by Govardhan & Williamson and by

Klamo et al. He explains the shortcomings of all previous damping parameters used in the study of VIV and then introduces a new damping parameter  $c^*$ , which is defined below.

$$c^* = 2c\omega/\rho U^2$$

By far the most interesting result to follow from his analysis, is that a very simple relationship is shown to exist between the lift coefficient,  $C_L$ , the dimensionless response amplitude,  $A^*$ , and the damping parameter, as shown in *Equation 1*:

$$C_L = A^* \cdot c^* \quad (1)$$

The key points from this analysis are repeated here because they not only provide great insight into the VIV problem but also help explain the strong Reynolds number dependence that Govardhan & Williamson (2006) and Klamo et al (2005) discovered and will be shown to exist with flexible cylinder data later on in this paper.

Starting with the equation of motion for a rigid, spring-mounted cylinder exposed to a cross flow,

$$\begin{aligned} m\ddot{y} + c\dot{y} + ky &= \frac{1}{2}C_F\rho U^2 D \sin(\omega t + \varphi) \\ &= \frac{1}{2}C_F\rho U^2 D [\sin(\omega t) \cos(\varphi) + \cos(\omega t) \sin(\varphi)] \end{aligned}$$

and after substituting  $y=A \sin(\omega t)$  for the response, the resulting equation can be separated into two equations; the first describes the dynamic equilibrium between the stiffness and inertial terms

$$(k - m\omega^2)A = \frac{1}{2}C_F\rho U^2 D \cos(\varphi)$$

And the second describes the equilibrium between the damping force and the lift force

$$c\omega A = \frac{1}{2}C_F\rho U^2 D \sin(\varphi)$$

After rearranging this equation, the relationship shown in *Equation 1* is obtained for the lift coefficient:

$$A^* \equiv \frac{A}{D} = \frac{\rho U^2}{2c\omega} C_F \sin(\varphi) = \frac{1}{c^*} C_F \sin(\varphi) = \frac{C_L}{c^*}$$

It is a well known fact that the Reynolds number influences the lift coefficient of stationary cylinders (Norberg, 2003). Klamo et al (2005) and Govardhan & Williamson (2006) showed that  $A^*$  is very dependent on Reynolds number for spring-mounted, rigid cylinders. *Equation 1*, from Vandiver (2012) makes it clear that the Reynolds number effect on  $A^*$  for rigid oscillating cylinders is entirely embodied in the lift coefficient, because  $c^*$  is composed only of parameters that have no Reynolds number dependence.

At this point *Equation 1* becomes extremely useful, because it allows the calculation of the lift coefficient from quantities that both Govardhan & Williamson (2006) and Klamo et al (2005) measured in their experiments. Namely, for every damping value tested, there is a corresponding peak  $A^*$  achieved by the vibrating cylinder. After calculating the  $c^*$

corresponding to each damping value it is then straightforward to calculate the  $C_L$  using *Equation 1*.

Doing so, one creates curves of  $C_L$  vs  $A^*$ , at a specific value of reduced velocity ( $V_r$ ), very similar to those used in VIV prediction software like SHEAR7 and VIVANA.

The  $C_L$  versus  $A^*$  curves created using the data from Govardhan & Williamson (2006) and Klamo et al (2005) are shown in *Figure 1a* and *1b* respectively.

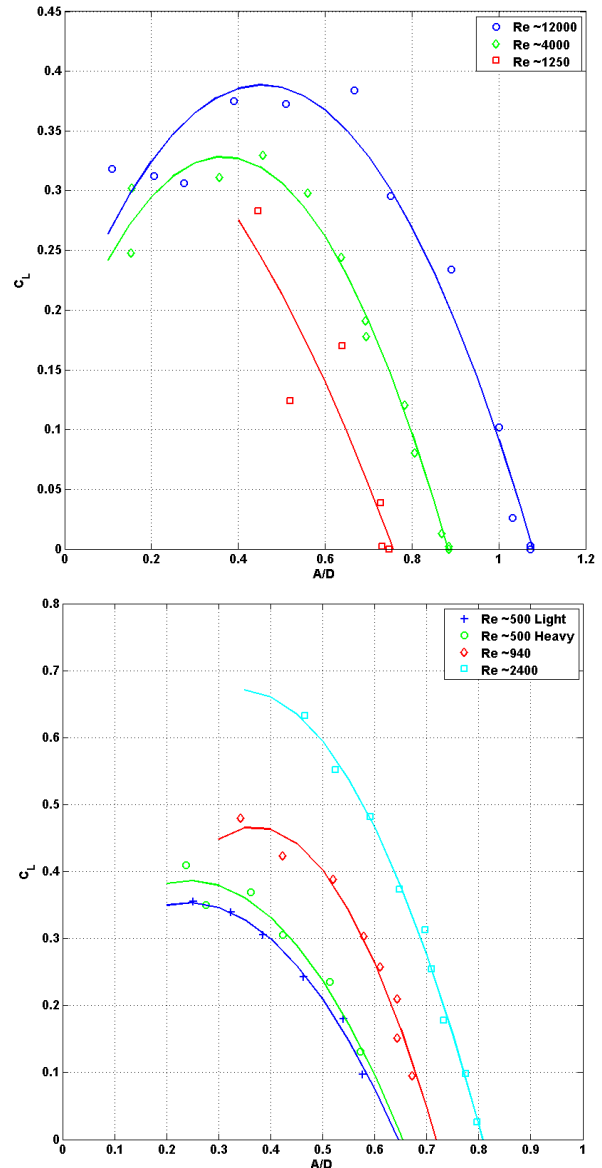


Figure 1  $C_L$  vs  $A/D$  at various Reynolds numbers  
**1a (top)** created using data from the experiments of Govardhan & Williamson (2006)  
**1b (bottom)** created using data from the experiments of Klamo et al (2005)

The keen observer will notice that even though the shape of the curves is very similar, the  $C_L$  values are quite different. This is due to differences in experimental setups such as aspect ratio, end plates etc. Despite this, it is very obvious that

in these Reynolds number ranges, increasing Reynolds number increases the magnitude of the lift coefficient.

The authors believe that the Reynolds number effect on  $A/D$  is best explained through the effect that Reynolds number has on the lift coefficient. The purpose of this paper is to show that a similar dependence of  $A/D$  on Reynolds number may be observed in the VIV response of flexible cylinders.

### 38m SHELL DATA

The 38m SHELL experiments were conducted at MARINTEK's ocean basin on behalf of SHELL International Exploration and Production Co. The experiment involved towing three densely instrumented flexible pipes, of different diameters, in uniform and sheared currents. The full test matrix included runs which tested the effects of fairings, strakes, staggered buoyancy and marine growth on riser response. The most interesting feature of this data set was the very large range of Reynolds numbers covered while testing the three different pipes. Towing velocities ranged from 0.25m/s to 3.45m/s which correspond to Reynolds number range from 5,000 to 220,000. More details on the experimental set-up can be found in OMAE2012-84055.

The properties of the three different pipes are summarized in Table 1. (MARINTEK, 2011)

Table 1. Pipe Properties

	Pipe 1	Pipe 2	Pipe 3
Length	38 m	38 m	38 m
Outer Diameter (Hydrodynamic Dia.)	12 mm	30mm	80 mm
Optical Diameter (Strength Diameter)	10 mm	27 mm	27 mm
Inner Diameter	(solid rod)	21 mm	21 mm
EI	16.1Nm <sup>2</sup>	572.3 Nm <sup>2</sup>	572.3 Nm <sup>2</sup>
E	3.27e10 N/m <sup>2</sup>	3.46e10 N/m <sup>2</sup>	3.46e10 N/m <sup>2</sup>
Mass in air (with contents)	0.197 kg/m	1.088 kg/m	5.708 kg/m
Mass in water (with contents)	0.078 kg/m	0.579 kg/m	0.937 kg/m
Mass ratio	1.74	1.54	1.14

The smallest pipe was instrumented with 52 Fiber Optic Bragg Strain gauges measuring pipe curvature in each of the cross-flow (CF) and in-line (IL) directions. The optical fiber was located at a distance of 5mm from the neutral axis and was covered by a silicon sheet 1mm thick. The medium and largest diameter pipe had curvature measured at 30 different locations and accelerations at 22 points in both the CF and IL directions. The largest diameter pipe was simply the medium sized pipe with a clam-like plastic shell, 25mm thick, surrounding it. For the medium and large pipes the curvature was measured at a distance of 13.5mm from the neutral axis and was covered by a silicon sheet 1.5mm thick.

Damping tests conducted in air for all three pipes yielded structural damping ratios of ~0.5-0.7% of critical damping.

Data will also be drawn from a set of runs where the largest diameter pipe was covered in P40 sandpaper in order to alter its surface roughness.

Analysis of the recorded data revealed the strong presence of higher harmonics in most of the test cases. All of the time-series data used in this work were band-pass filtered around the 1X or 2X response frequencies for the CF and IL directions respectively. Thus the 3X, 4X and 5X components are excluded from the data shown here.

### ANALYSIS

The variables under investigation in this paper are:

#### The Strouhal number

$$St = \frac{f_{response} D}{U}$$

The Strouhal number for each test was calculated by identifying the resonant frequency,  $f_{response}$ , from the response spectrum of several curvature sensors within the power-in region.

#### Response amplitude

For the medium and large sized pipes, the amplitude at every accelerometer location was determined after integrating the accelerometer time history in the frequency domain. For the smallest pipe, the response amplitude was determined after reconstructing the displacement response based on the measured curvature and identifying the mode weights.

In all cases, once the response amplitude was known, the spatial mean of the RMS values in time,  $\overline{\sigma_{A/D}}$ , was calculated according to:

$$\overline{\sigma_{A/D}} = \frac{\sum_{i=1}^N \sqrt{\sigma_{A/D}}}{N} = \frac{\sum_{i=1}^N \sqrt{\frac{1}{M} \sum_{j=1}^M (y_j - \bar{y})^2}}{N D}$$

Where  $N$  is the number of sensors and  $M$  is the number of samples in the time history under consideration.  $y_j$  and  $\bar{y}$  are respectively the instantaneous amplitude and the mean value in time at a specific sensor.

Even though the above parameter is useful when looking at data from uniform flow tests, it should not be used with response data from sheared flow tests. Sheared flow tests usually have large response amplitudes within the power-in region but the response outside the power-in region is considerably smaller. Therefore averaging the response amplitude over the entire riser length is not appropriate. Instead, the maximum RMS value,  $\sigma_{A/D}^{MAX}$ , along the length is a more appropriate metric.

To account for the possibility, that the location where the maximum response occurs, falls between two measurement locations, a modal reconstruction along the lines of Lie & Kaasen (2006) was performed for each case. The appendix contains an example of a typical case.

#### Drag coefficient

The drag coefficient along the length of the pipe was estimated based on the method outlined in Jhingran et al (2008). The key points are repeated below. Starting with the equation of motion in the IL direction:

$$(m(x) + m_a(x, \omega)) \frac{\partial^2 y}{\partial t^2} + c(x) \frac{\partial y}{\partial t} + (EI(x) \frac{\partial^4 y}{\partial x^4} - T(x) \frac{\partial^2 y}{\partial x^2}) = F(x, t)$$

Taking the temporal mean,  $\overline{(\quad)^t}$ , makes all zero-mean terms vanish. If  $EI$  is neglected for a tension dominated riser, the above formula simplifies to:

$$-T(x) \frac{\partial^2 y}{\partial x^2} = \overline{F(x)^t}$$

The force term on the RHS is simply the drag force per unit length, which can be expressed as:

$$F(x) = \frac{1}{2} C_D(x) \rho D U(x)^2$$

Substituting and rearranging yields the drag coefficient  $C_D$ .

$$C_D(x) = \frac{4 T(x) \frac{\partial^2 y}{\partial x^2}}{\rho D U(x)^2}$$

It is important to emphasize that all these quantities are calculated locally (i.e. at a specific sensor, located at a distance  $x$  from the end), and as such the drag coefficient will vary considerably along the length of the riser.

### Power-in location

The power-in region is traditionally defined as the region along the length of the pipe where the wake is well correlated with the riser motion.

In uniform flow tests when the pipe is responding at low mode numbers the power-in region extends over the entire riser length. Since, the entire pipe is exposed to the same current, determining the corresponding Reynolds number for such a case is straightforward.

The same cannot be said for sheared flows though. Here, the current varies along the pipe length, and as such the Reynolds number varies from 0 on one end to  $\frac{U_{max} D}{\nu}$  on the high velocity end. The question that then arises is: what's the appropriate Reynolds number for such a case?

Choosing the Reynolds number that corresponds to the location of the power-in region seems like a sensible choice. Identifying the power-in region in sheared flows is still a matter of current research, yet one can try to use previous experimental evidence to approximately identify this region.

VIV experiments on flexible cylinders in sheared and non-uniform currents, such as the Lake Seneca tests, the Miami II tests, the 38m NDP tests as well as the current SHELL tests typically show that the largest strains are always near the high velocity end and the response decays as you move toward the low velocity end (see *Figure A1* in the Appendix).

The exact location of the power-in region will eventually depend on which mode -of all the potentially excited modes- ends up dominating the response. In this work, it will be assumed that the power-in region is approximately centered at a distance  $x/L=0.25$  away from the high velocity end. Accordingly, the Reynolds number for the sheared flow cases, to be used in the comparisons later on, will be 25% smaller than the maximum Reynolds number which is always at  $x/L=0$ .

The trends between the response amplitude and the Reynolds number for the sheared flow cases are not very sensitive to the precise location at which the Reynolds number is computed, which in this paper is at  $x/L=0.25$ . If a slightly larger or smaller Reynolds number had been chosen the data on a plot of  $A/D$  vs  $Re$  would simply shift slightly to the right or left respectively and all trends in the plots of  $A/D$  vs  $Re$  would appear the same.

## RESULTS

*Table 2* summarizes some of the key results from the tests. The Reynolds number reported for the sheared flow tests is the value corresponding to what is believed to be the power-in region and not the maximum Reynolds number on the riser.

**Table 2 Range of values for all tests cases under review.**

	Reynolds #	Mode #	$\overline{\sigma_{A/D}}$	$\sigma_{A/D}^{MAX}$	$n \zeta$
Pipe 1 Uniform	4.9e3 – 3.76e4	10 – 26	0.32 – 0.52	0.47 – 0.84	0.07 – 0.18
Pipe 1 Shear	4.1e3 – 2.54e4	9 – 30	0.26 – 0.36	0.39 – 0.49	
Pipe 2 Uniform	6.6e3 – 6.8e4	3 – 11	0.30 – 0.57	0.42 – 0.83	0.02 – 0.08
Pipe 2 Shear	6.2e3 – 5.9e4	3 – 13	0.27 – 0.47	0.36 – 0.71	
Pipe 3 Uniform	3.6e4 – 1.3e5	2 – 7	0.39 – 0.64	0.54 – 0.91	0.01 – 0.05
Pipe 3 Shear	2.7e4 – 1.6e5	2 – 8	0.36 – 0.62	0.49 – 0.81	
Rough Uniform	1.8e4 – 1.2e5	2 – 7	0.31 – 0.48	0.46 – 0.73	0.01 – 0.05
Rough Shear	4.9e4 – 1.5e5	4 – 11	0.31 – 0.40	0.39 – 0.50	

*Figure 2* shows how the response amplitude of the medium sized pipe varied as a function of Reynolds number. The plot shows the spatial mean ( $\overline{\sigma_{A/D}}$ ) and maximum ( $\sigma_{A/D}^{MAX}$ ) in both the *CF* and *IL* amplitudes for all the uniform flow cases. The influence that Reynolds number has on the response data is clearly visible, with the response amplitude in both *CF* and *IL* directions increasing as the Reynolds number is increased.

If one assumes that the power-in region for uniform flow covers the entire riser length, then there is no hydrodynamic damping present, and the only damping present in the system is the structural/hysteretic damping which is the same for all cases.

Since all other factors are the same, the scatter can be attributed to variations in reduced velocity. This is further reinforced by the fact that at the larger Reynolds numbers (and hence higher velocities and higher excited mode numbers) the scatter is smaller. At high mode numbers the natural frequencies are spaced much closer than at low mode numbers, which means that there is a higher probability that the selected towing speed will coincide or be very close to that mode's critical reduced velocity.

*Figure 3* shows how the Strouhal number, determined from the uniform flow tests, varies as a function of the Reynolds number. Looking at the bare cylinder data, it is obvious that the Strouhal number decreases as the Reynolds number increases.

A best fit through all of the bare pipe data (i.e. excluding the roughened pipe) presented in *Figure 3* in the Reynolds range investigated is:

$$St = -0.0065 \ln(Re) + 0.21$$

*Figure 4* shows the spatial mean RMS amplitude,  $\overline{\sigma_{A/D}}$ , in the CF and IL directions for all the pipes tested in this experiment. The figure also shows Swithenbank's best fit from her 2008 paper.

The first thing to point out here is the peculiar behavior seen in the CF response of Pipe 1. Initially, the response amplitudes are large but at Reynolds numbers greater than 17-18k the response amplitude starts decreasing rapidly. This is most likely attributed to the very high response mode (20+) and correspondingly high  $n\zeta$  values which typically indicate strong traveling wave response and/or strong response attenuation outside the power-in region. The  $n\zeta$  values for the smallest pipe are more than twice as large as the Pipe 2 values and close to four times larger than the values that correspond to Pipe 3.

This sudden change in the response characteristics is consistent with the dynamic behavior changing from a predominantly standing wave response to a strong travelling wave response. The reasons why this happens so suddenly are not clear, but in any case, this behavior is not believed to be a Reynolds number effect, but is more likely due to the difference in VIV response, which is dominated by travelling waves at high mode numbers and standing waves at low mode numbers. The response data from Pipe 1 will not be considered when calculating curve fits for the  $A/D$  vs  $Re$  data.

The relatively large scatter in the CF RMS  $A/D$  values of Pipe 3 is due to the fact that the responding modes are much lower (3-7) and a lot of the variability can be attributed to reduced velocity effects.

The best fits through the bare Pipe 2 and Pipe 3 data for the CF and IL direction are:

$$CF \text{ direction: } \overline{\sigma_{A/D}} = 0.077 \ln(Re) - 0.343$$

$$IL \text{ direction: } \overline{\sigma_{A/D}} = 0.023 \ln(Re) - 0.087$$

In *Figure 5*, note how the maximum RMS response amplitudes,  $\sigma_{A/D}^{MAX}$ , for the sheared cases are always smaller than the uniform flow cases. This happens because under sheared flow conditions the power-in length is limited to a small portion of the riser and the remaining sections provide hydrodynamic damping. As a result, the sheared flow cases always have higher damping values than their corresponding uniform flow cases. The increased damping will in turn limit the maximum resonant amplitude.

The best fit through the data for the CF direction is:

$$CF \text{ direction: } \sigma_{A/D}^{MAX} = 0.101 \ln(Re) - 0.440$$

Once again, the roughened pipe data was not included when calculating this fit and neither was the Pipe 1 data since it exhibited different dynamic behavior.

*Figure 6* shows the spatial mean drag coefficient,  $C_d$ , along the riser length calculated from the uniform flow cases.

Little emphasis has been placed until this point on the results of the *roughened cylinder*; it has been included here to demonstrate how profoundly the surface roughness can alter the response characteristics. The roughened cylinder results are directly comparable with the large diameter (Pipe 3) results since all other properties (aspect ratio,  $Re$ , etc) are the same. From *Figure 3* it is apparent that the Strouhal number is considerably larger for the rough pipe, whereas *Figure 4* reveals that the response amplitude in both CF and IL directions is significantly smaller than its bare cylinder counterpart.

*Figure 7* shows the drag coefficient at **every location** along the riser as a function of the Reynolds number at that location. Only the data corresponding to the largest diameter pipe with and without the rough surface finish has been included.

At a given Reynolds number the variation in  $C_d$  is due to the  $A/D$  dependence, especially obvious when looking at the uniform flow results, which show a lot of scatter consistent with the variation in  $C_d$  seen at the nodes or anti-nodes of a strong standing wave response.

At Reynolds numbers smaller than  $10^5$  there is a lot of overlap in the  $C_d$  values shown. As Reynolds number increases, well into the drag crisis region, the  $C_d$  for the smooth pipe starts decreasing whereas the  $C_d$  for the roughened pipe is considerably larger.

## CONCLUSIONS

The first part of this paper provides an explanation for the strong influence of Reynolds number on the response of rigid cylinders vibrating freely in a cross-flow. This is attributed to the effects that Reynolds number has on the lift coefficient, demonstrated here, using the experimental data from Govardhan & Williamson (2006) and Klamro et al (2005).

The most interesting result from the analysis of the SHELL 38m long data, is the clearly demonstrated effect that increasing Reynolds number has on the response amplitude of flexible cylinders. The trend identified is in good agreement with what has been previously reported for flexible cylinders and there are strong similarities with the effect of Reynolds number on rigid cylinders. For elastically mounted rigid cylinders vibrating in a cross flow, this work shows that the lift coefficient increases as the Reynolds number is increased. The same should hold true for the lift coefficient of flexible risers.

Many of the factors that influence the response of rigid cylinders are also important for the response of flexible cylinders. A lot of the scatter seen in the plotted results- in this work and in previous studies- can be attributed to variations of these parameters between experiments. The most notable are damping, reduced velocity, aspect ratio and responding mode number as well as surface roughness.

The Strouhal number for a vibrating riser decreases as the Reynolds number is increased, approaching a limiting value between 0.13 and 0.14 at Reynolds numbers up to  $1.4 \times 10^5$ . This is a very interesting result because Strouhal number data from stationary cylinders in the same Reynolds number range show that it remains roughly constant at  $\sim 0.18$ -0.2 from  $Re \sim 500$  until the drag crisis region around  $Re \sim 2 \times 10^5$ . This has important implications for riser designers, since a lower Strouhal number at a given Reynolds number will typically mean a lower excited mode and hence smaller strains for a given current speed.

Further experimental evidence, at even higher Reynolds numbers, is necessary to see if this limiting value will hold even beyond the drag crisis regime.

## ACKNOWLEDGEMENTS

The authors acknowledge the SHEAR7 JIP members (Amog Consulting, BP, Chevron, ExxonMobil, Petrobras, Shell, Statoil & Technip) for supporting this research and Shell International Exploration and Production for providing the data. Special thanks are due to Mr. Zhibiao Rao for his assistance with the response reconstruction methodology.

## REFERENCES

MARINTEK, 2011, *Shell Riser VIV Tests Main Report*, No. 580233.00.0

Govardhan, R.N. & Williamson, C.H.K., 2006, *Defining the Modified Griffin Plot in Vortex-Induced Vibration: Revealing the Effect of Reynolds Number Using Controlled Damping*, Journal of Fluid Mechanics 561, 147-180

Klamo, J.T, Leonard, A. & Roshko, A., 2005, *On the Maximum Amplitude of a Freely Vibrating Cylinder in Cross-Flow*, Journal of Fluids and Structures 21, 429-434

Swithenbank, S.B., Vandiver, J.K., Larsen, C.M. & Lie, H., 2008, *Reynolds Number Dependence of Flexible Cylinder VIV Response Data*, OMAE2008-57045

Vandiver, J.K., 2012, *A Damping Parameter for Flow Induced Vibration*, Journal of Fluids and Structures (under review)

Jhingran V., Jaiswal, J. & Vandiver, J.K., 2008, *Spatial Variation of Drag on Long Cylinders in Sheared Flow*, OMAE2008-57803

Lie, H. & Kaasen, K.E., 2006, *Modal Analysis of measurements from a large scale VIV model of a riser in a linearly sheared flow*, Journal of Fluids and Structures 22, 557-575

Norberg, C., 2003, *Fluctuating Lift on a Circular Cylinder: Review and New Measurements*, Journal of Fluids and Structures 17, 57-96

Lie, H. et al, 2012, *Comprehensive Riser VIV Model Tests in Uniform and Sheared Flow*, OMAE2012-84055

## NOMENCLATURE

$A$	Response amplitude
$A^*$	Dimensionless response amplitude
$c$	Damping coefficient per unit length
$C_L$	Lift coefficient
$C_d$	Drag coefficient
$D$	Hydrodynamic diameter
$EI$	Bending stiffness ( $N\ m^2$ )
$f_{response}$	Response frequency (Hz)
$k$	Stiffness per unit length
$L$	Pipe length (m)
$m$	Mass per unit length
$m_a$	Added mass per unit length
$n$	Mode number
$Re$	Reynolds number
$St$	Strouhal number
$T$	Axial tension (N)
$U(x)$	Current (m/s) at position $x$
$U_{MAX}$	Maximum current (m/s) along pipe
$V_r$	Reduced velocity
$x$	Position along riser (m)
CF	Cross-Flow direction
IL	In-Line direction
$\zeta$	Damping ratio
$\nu$	Kinematic viscosity
$\rho$	Density
$\sigma_{A/D}^{MAX}$	Spatial maximum RMS A/D
$\overline{\sigma_{A/D}}$	Spatial mean RMS A/D
$\omega$	Response frequency (rad/s)

## APPENDIX

### Example of Response Reconstruction for a Sheared flow case

Figure A1 is a typical example of the response of a riser in a sheared flow. The test run is number 3112, which involved towing the medium sized pipe ( $\Phi=0.03\text{m}$ ) in a sheared current with a maximum speed of  $1.5\text{m/s}$  at  $x/L=0$ . The maximum Reynolds number is  $\sim 40900$  but the Reynolds number corresponding to the power-in region will be somewhat smaller. The blue stars indicate the measured quantities, while the continuous green curves represent the modal reconstruction. The maximum response is on the high velocity end of the riser, but the location of the power-in region is not immediately apparent.

Figure A2 shows the drag coefficient  $C_d$  at every curvature sensor along the riser. The data presented in this plot is typical of the data used to create Figure 7, where all the test cases (Pipe 3 and Pipe 3 Rough) and all the sensor data have been included.

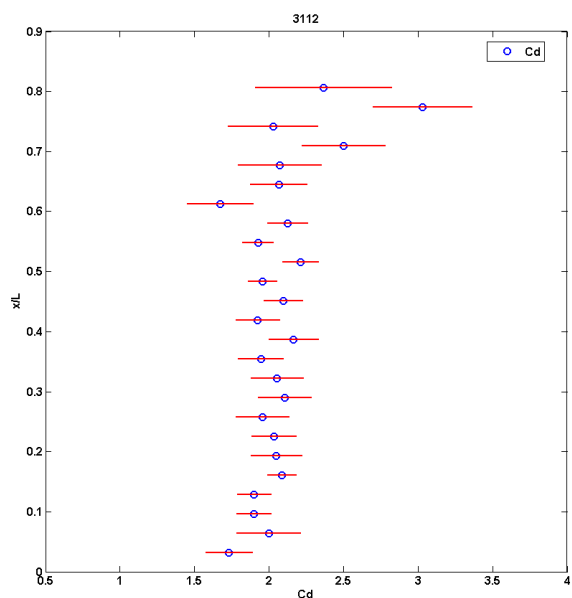


Figure A2 Drag Coefficient as a function of  $x/L$  for test 3112. The red lines indicate the uncertainties in the  $C_D$  calculation at every measurement location

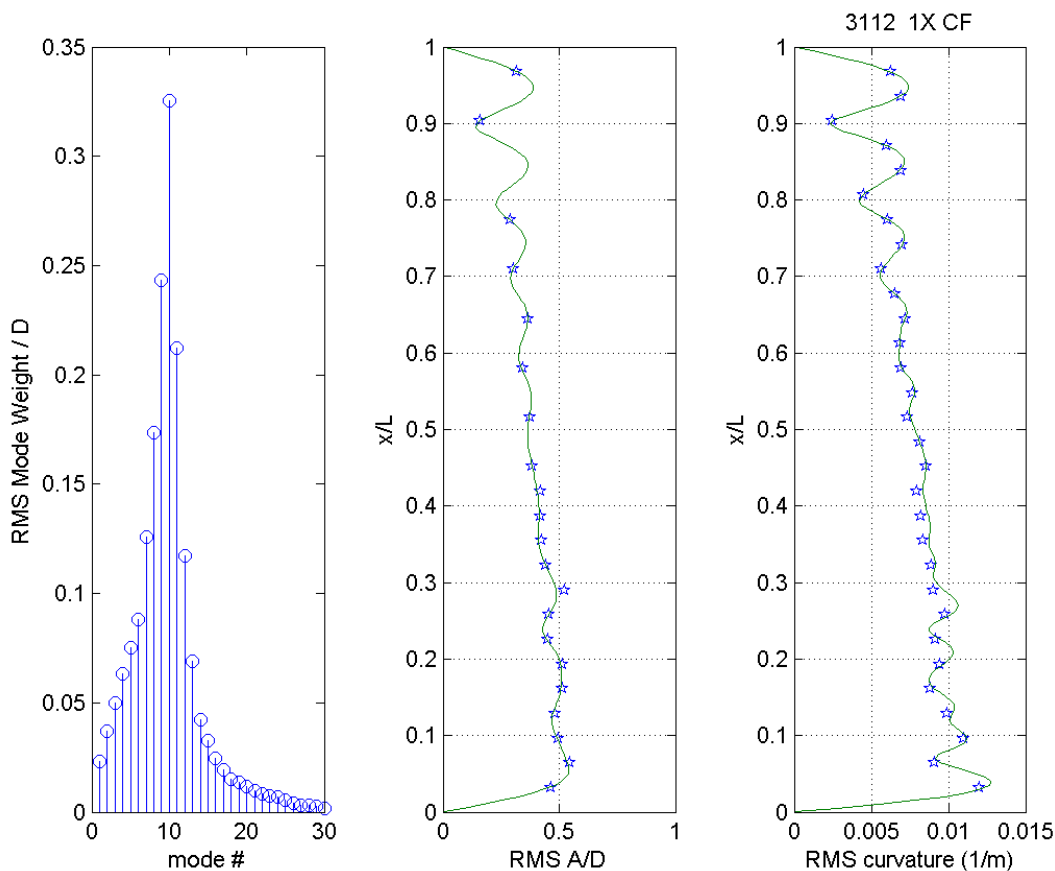


Figure A1

Plot of CF response for test 3112



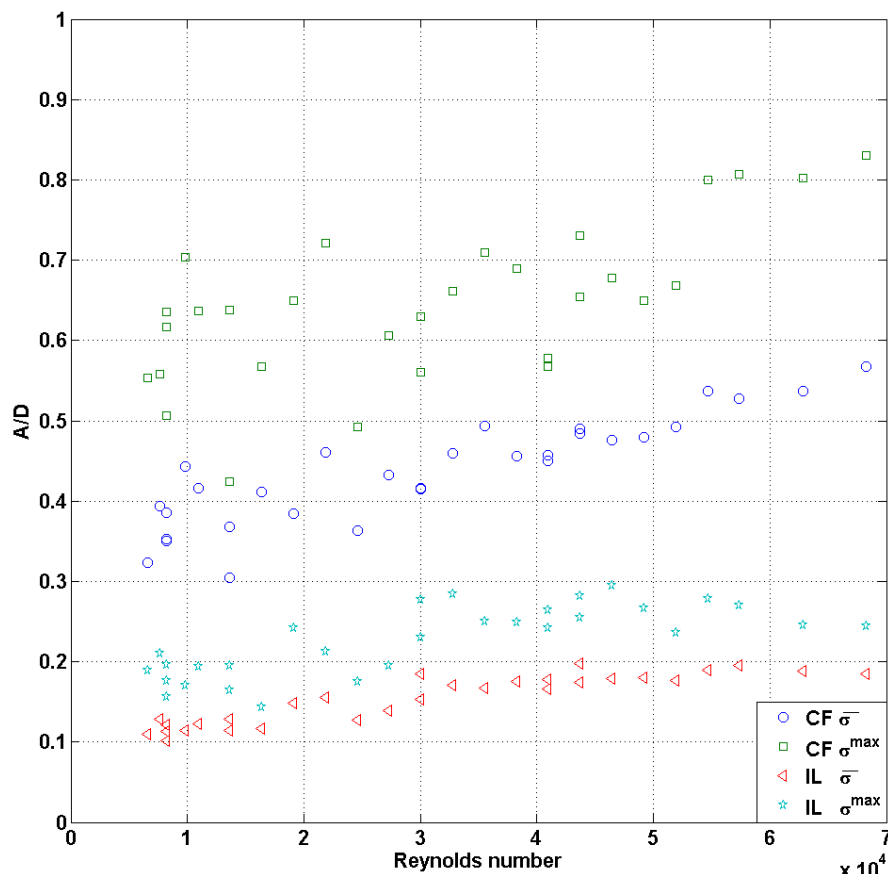


Figure 2 A/D response vs Reynolds number for Pipe 2 in uniform flows

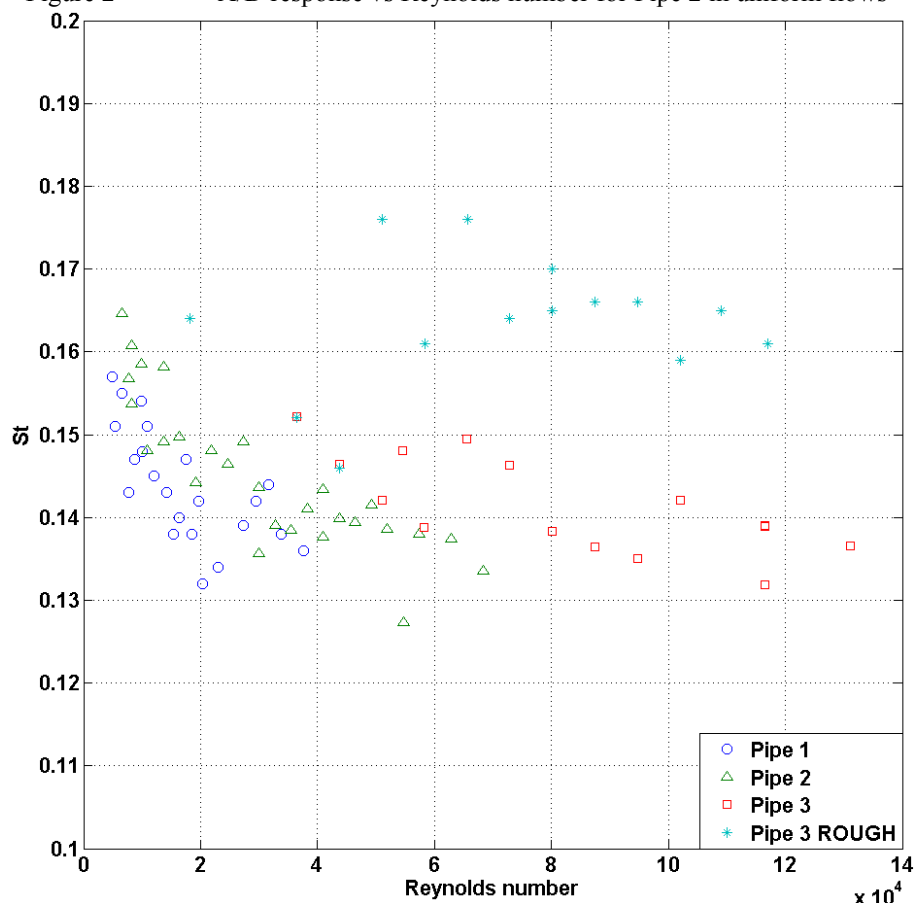


Figure 3 Strouhal number vs Reynolds number from uniform flow tests

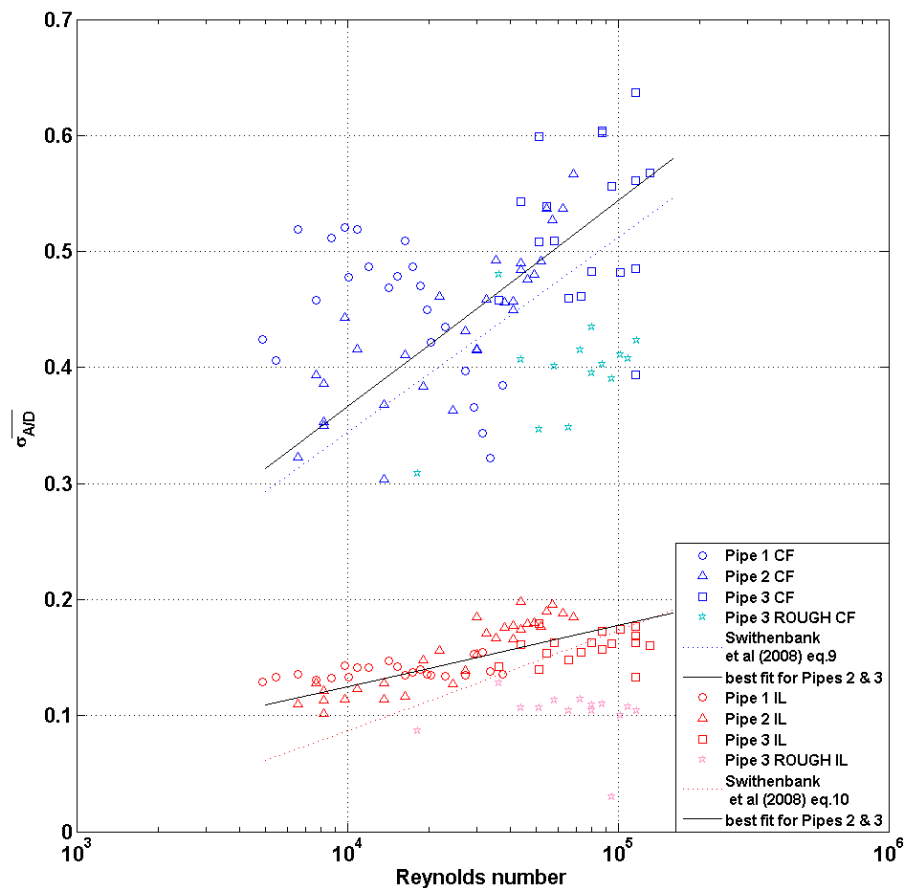


Figure 4  $\overline{\sigma_{A/D}}$  vs Reynolds number for the CF and IL directions in uniform flows

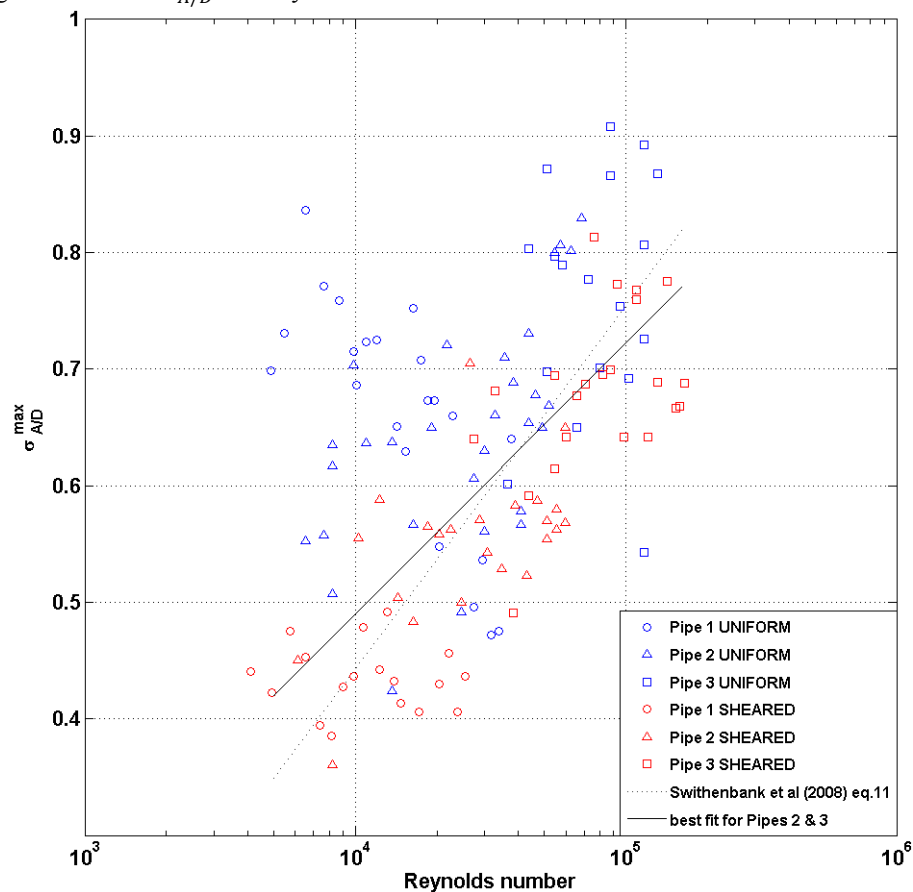


Figure 5 Cross-flow  $\sigma_{A/D}^{MAX}$  vs Reynolds number for uniform and sheared flows

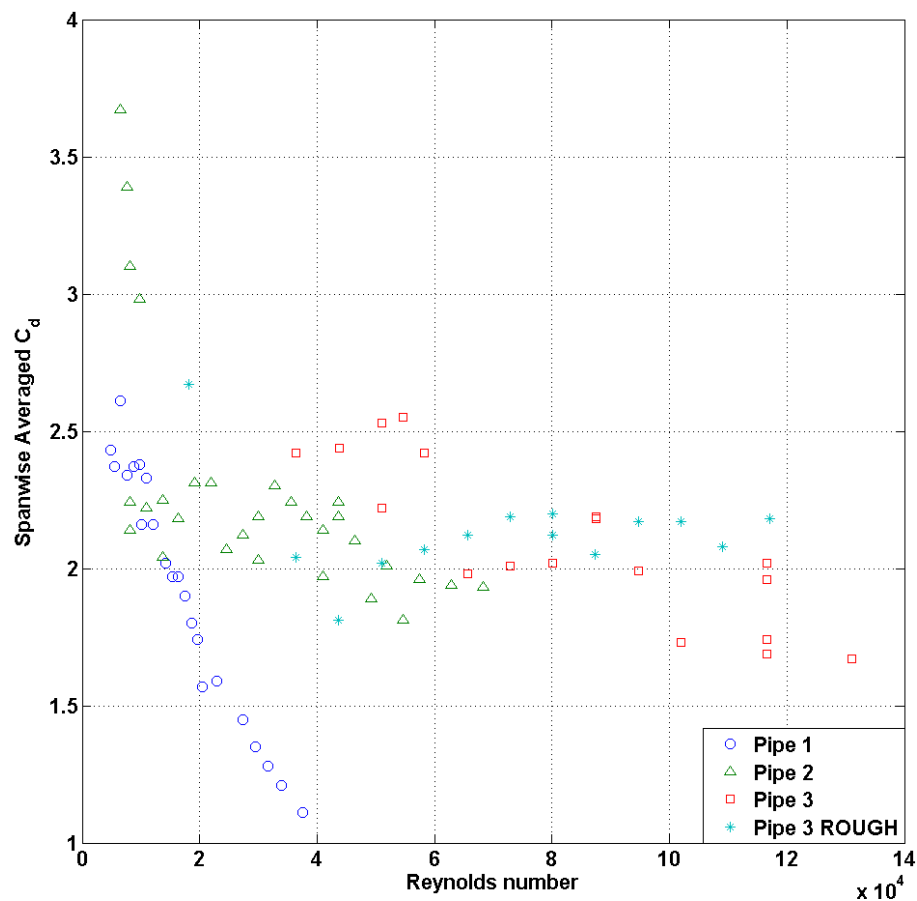


Figure 6 Spanwise averaged  $C_d$  vs Reynolds number from uniform flow tests

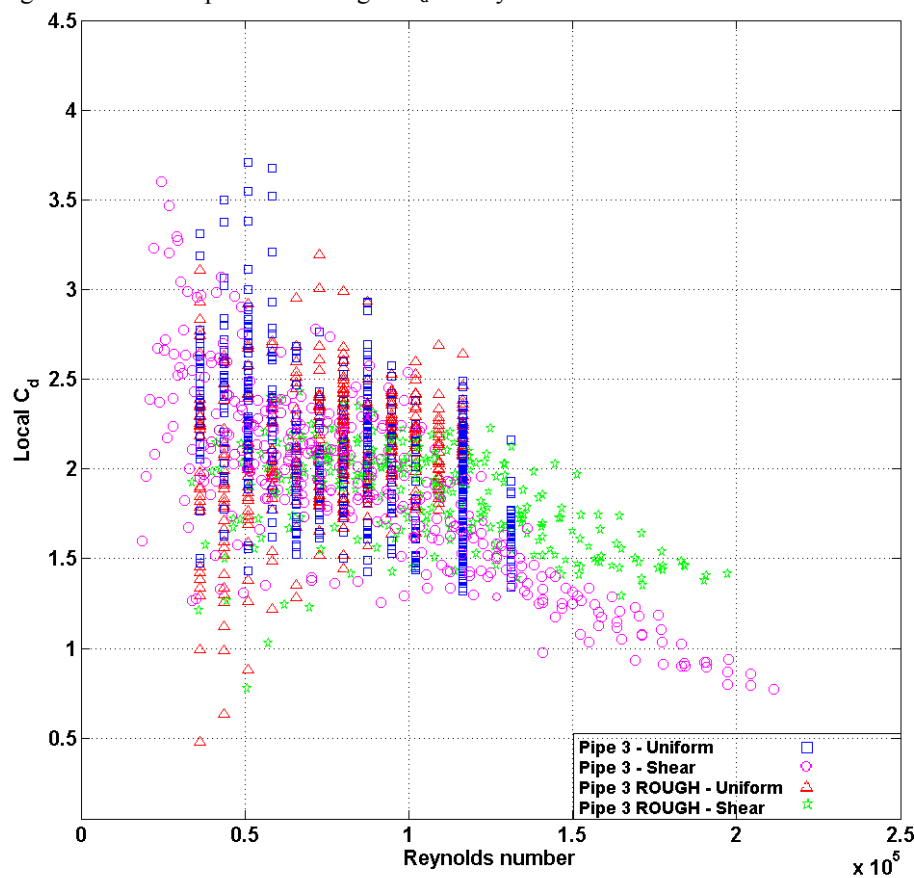


Figure 7 Local  $C_d$  vs Reynolds number for Pipe 3 (smooth and rough) in uniform and sheared flows